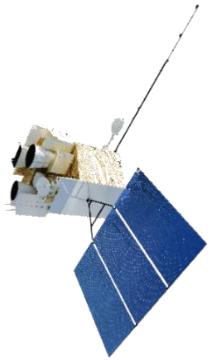

Pseudo-invariant pixels (PIPs) for sensor calibration

Junwei Wang, **Xiuqing Hu**

National Satellite Meteorological Center (NSMC), CMA

Vicarious calibration methods overview

Earth surfaces with suitable characteristics have long served as benchmark or test sites to verify the post-launch radiometric calibration performance of satellite instruments.

- Field campaigns on reference standard test sites (eg. Dunhuang, Railroad Valley Playa)
- Pseudo-invariant calibration sites (PICS)
- Ice or snow fields (Greenland, Dome C, Tibetan Plateau Glaciers)
- Deep convective clouds (DCC)
- Rayleigh scattering
- Liquid water cloud
- Sun glint
- The Moon
- The stars

- Pseudo-invariant Targets Selection based on prior knowledge
- Large, homogenous areas
- Types and quantities of these targets are limited, resulting in low calibration frequency and dynamic ranges

To achieve high-frequency, high-dynamic range, and high-precision in-orbit calibration of satellite sensors, we propose a pseudo-invariant pixels (PIPs) based strategy for sensor calibration (degradation trending and inter-calibration).

IR-MAD technique for PIPs selection

Image pairs

IR-MAD: iteratively re-weighted multivariate alteration detection (MAD)

- The IR-MAD technique was first proposed for change detection by Nielsen (1998,2007), and later used in the radiometric normalization [Canty et.al, 2004, 2008], radiometric calibration of AVHRR (Schmidt, 2008)
- Consider an image pair (**F**, **G**) composed of two images acquired at different times by the same sensor or images acquired simultaneously by two different sensors,

$$U = \mathbf{a}^{\mathrm{T}}\mathbf{F} = a_1F_1 + a_2F_2 + \ldots + a_NF_N$$

$$V = \mathbf{b}^{\mathrm{T}}\mathbf{G} = b_1G_1 + b_2G_2 + \ldots + b_NG_N$$

$$MAD_i = U_i - V_i = \mathbf{a}_i^{\mathrm{T}}\mathbf{F} - \mathbf{b}_i^{\mathrm{T}}\mathbf{G}, i=1,\ldots,N$$

- transform the image data to a feature space, which is more conducive to detect change or no-change in the scene. The MAD transformation is linear scale invariant under affine transformations, thus is insensitive to the differences in gain and offset settings of the sensor

$$Z = \sum_{i=1}^{N}\left(\frac{MAD_i}{\sigma_i}\right)^2 < k$$

- Pixels that meet this criterion are designated as pseudo-invariant pixels and can be used for calibration

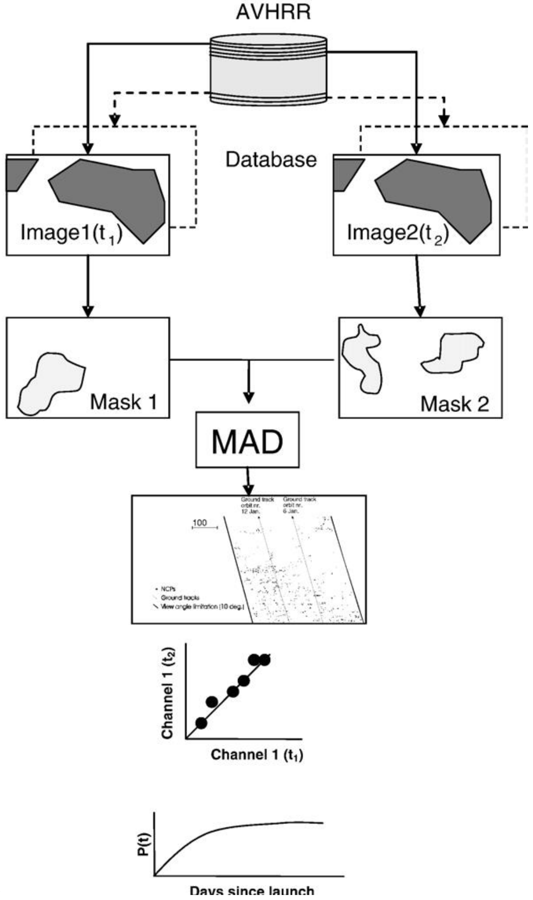

(Schmidt, 2008)

PART 01

Sensor degradation trending based on PIPs

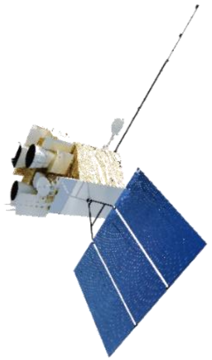

FY-3D/MERSI-II overview

Acronum	MERSI-II
Full name	Medium Resolution Spectral Imager – II
Purpose	Multi-purpose imagery, including ocean colour
Short description	25-channel VIS/IR spectro-radiometer
Background	Replacing and merging MERSI on FY-3A/3B and VIRR on FY-3A/3B/3C
Scanning Technique	Cross-track: 2048 samples for channels at 1000 m resolution at nadir, or 8192 samples for channels at 250 m resolution, swath 2900 km - Along-track: ten 1-km lines every 1.5 s.
Resolution	250 m or 1.0 km at s.s.p.
Coverage / Cycle	Global coverage once/day (VIS/NIR/SWIR channels), twice/day (MWIR/TIR).

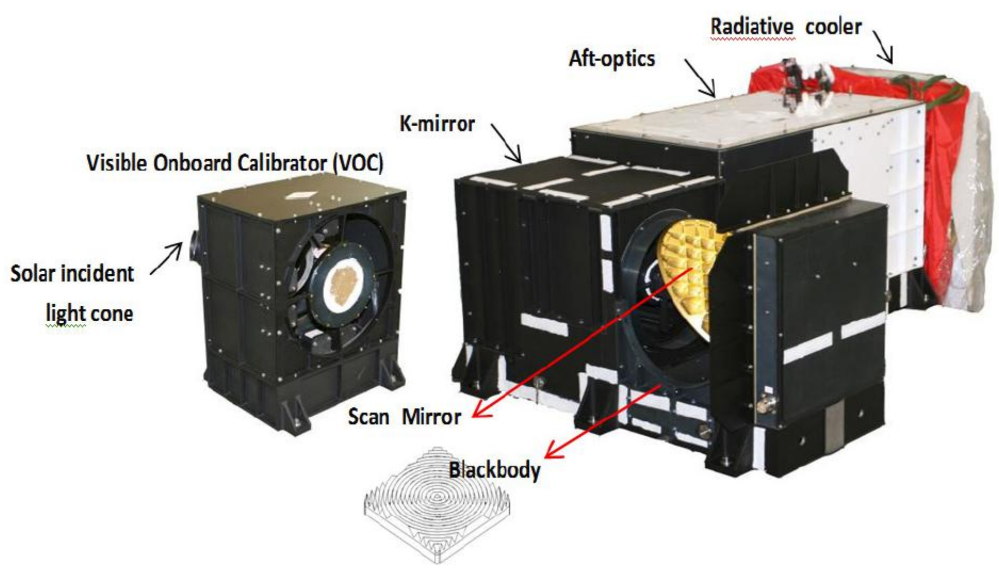

Relative Sensor degradation for single image pair

Analyze the PIPs location and the relative degradation of the sensor with two image pairs that have different acquisition time intervals.

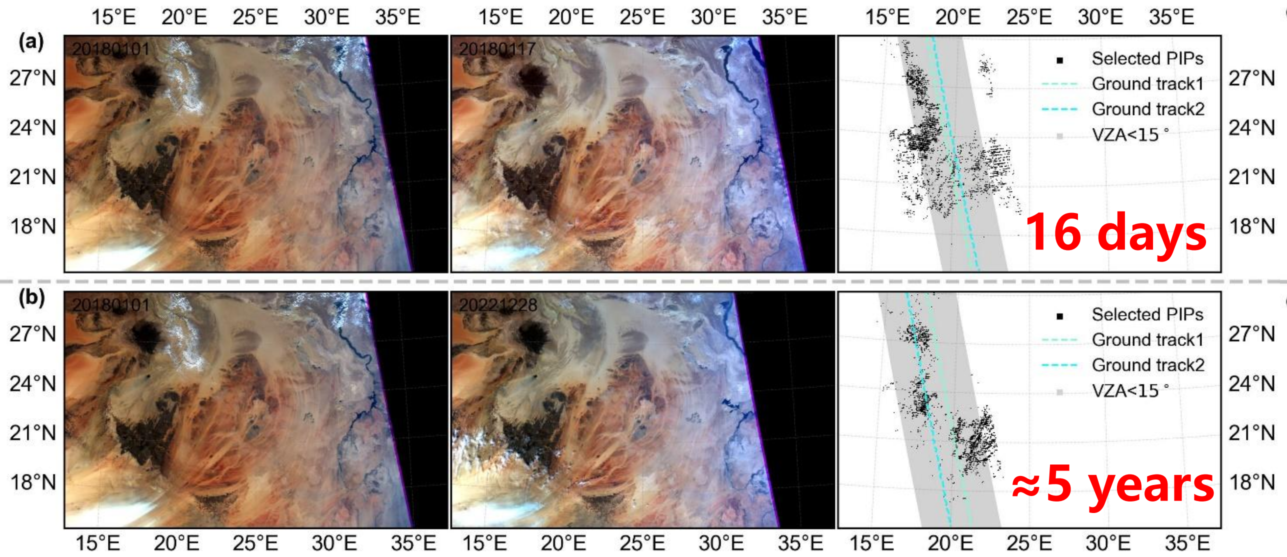

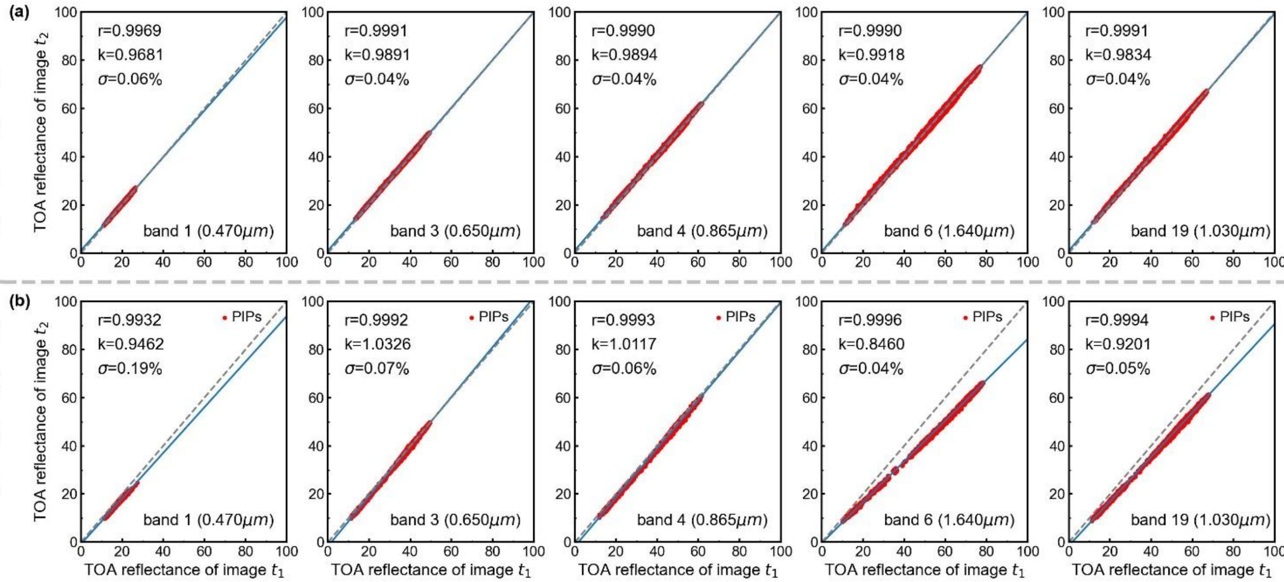

- The two image pairs show consistent spatial distributions of PIPs
- The regressions have high correlation, the slopes reflects the relative degradation of the sensor for each band over the time interval
- The PIPs reflect targets with high temporal stability, and aggregating them yields PICS

Long-term degradation trending for all image pairs

Construct image pairs and perform same PIPs analysis on all image pairs for long-term FY-3D/MERSI-II data from January 1, 2018, to August 31, 2023, spanning over five years.

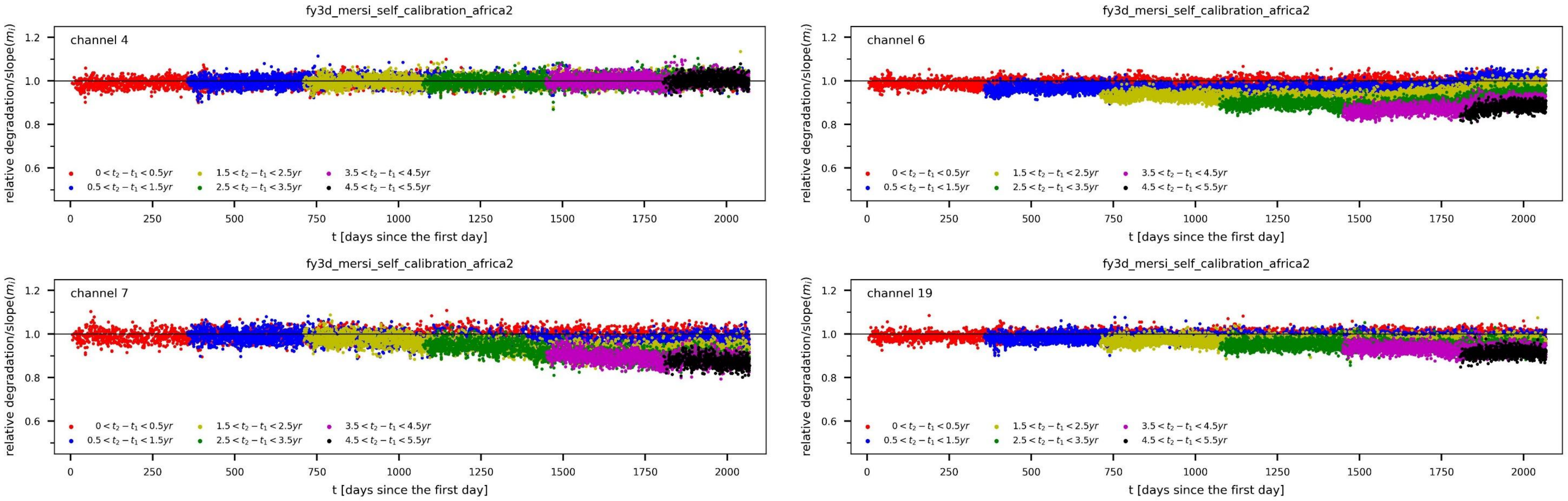

- The dots with different colors represent regression slopes from image pairs with different time intervals
- Image pairs with longer intervals exhibit more pronounced sensor degradation.

Comparison with other methods for long-term trends

Obtaining sensor degradation over time through polynomial fitting and comparing it with traditional degradation monitoring method

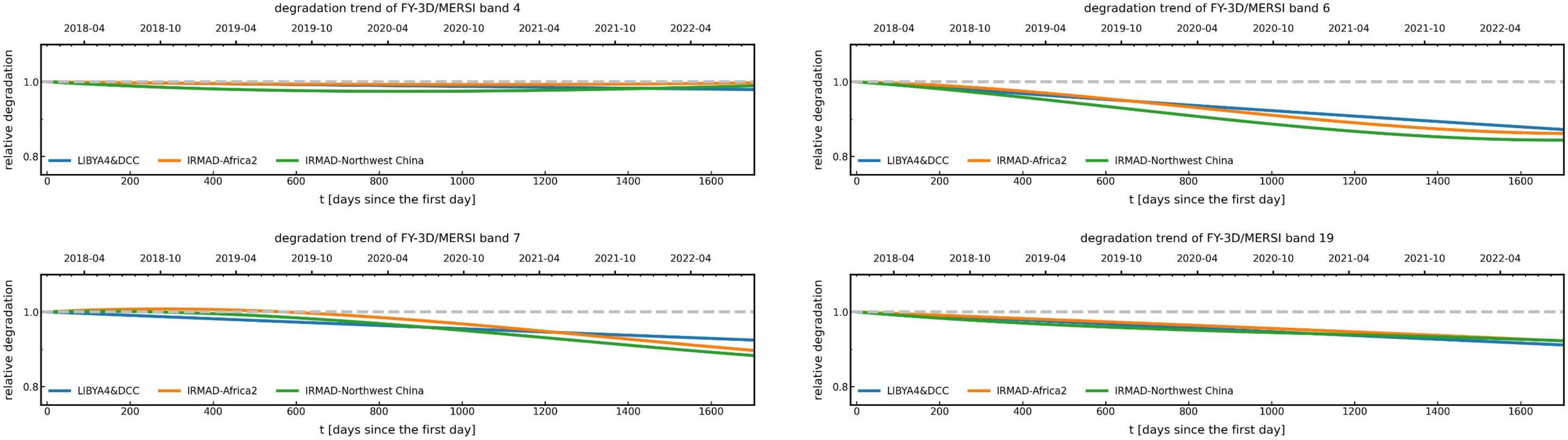

- Results of the PIPs based method are consistent with those from traditional PICS&DCC method
- The PIPs based method yields consistent results across different regions.

Normalization of the long-term regression slopes

For each band, normalize the regression slopes of each image pair using the fitted long-term degradation trends

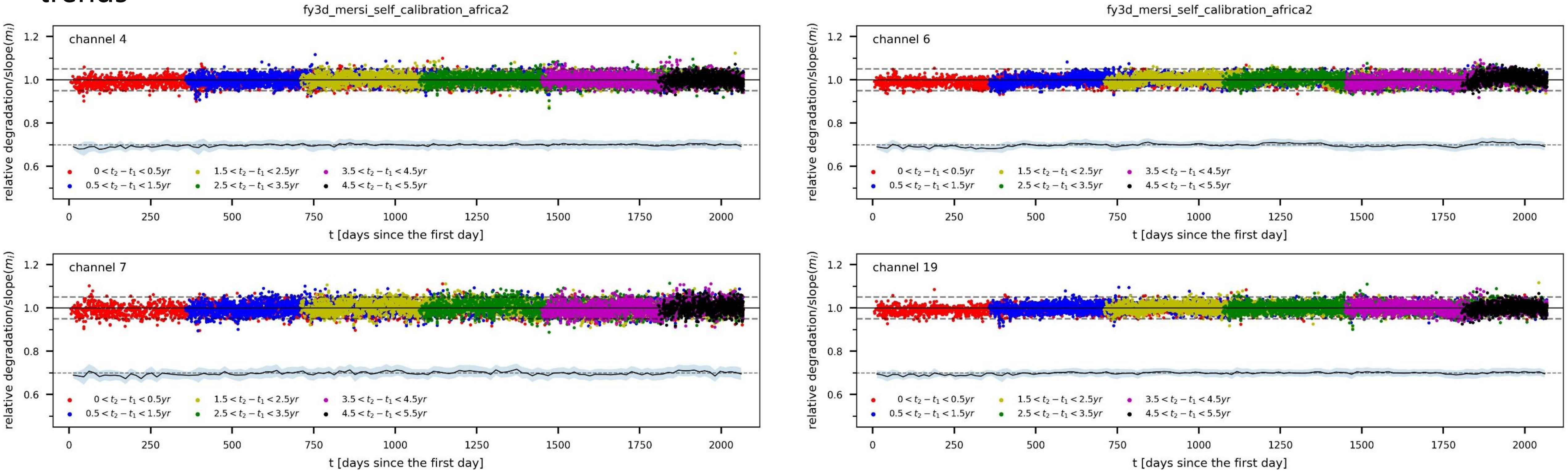

- After normalization, the regression slopes are distributed around 0.95-1.05 with a mean of 1, indicating that the instrument decay trend has been fitted well.
- The standard deviation represents the uncertainty of relative degradation for individual image pairs.

Analysis across global regions.

Analysis is conducted on nine global regions, comparing the results obtained from different regions and identifying global PIPs (GPIPs)

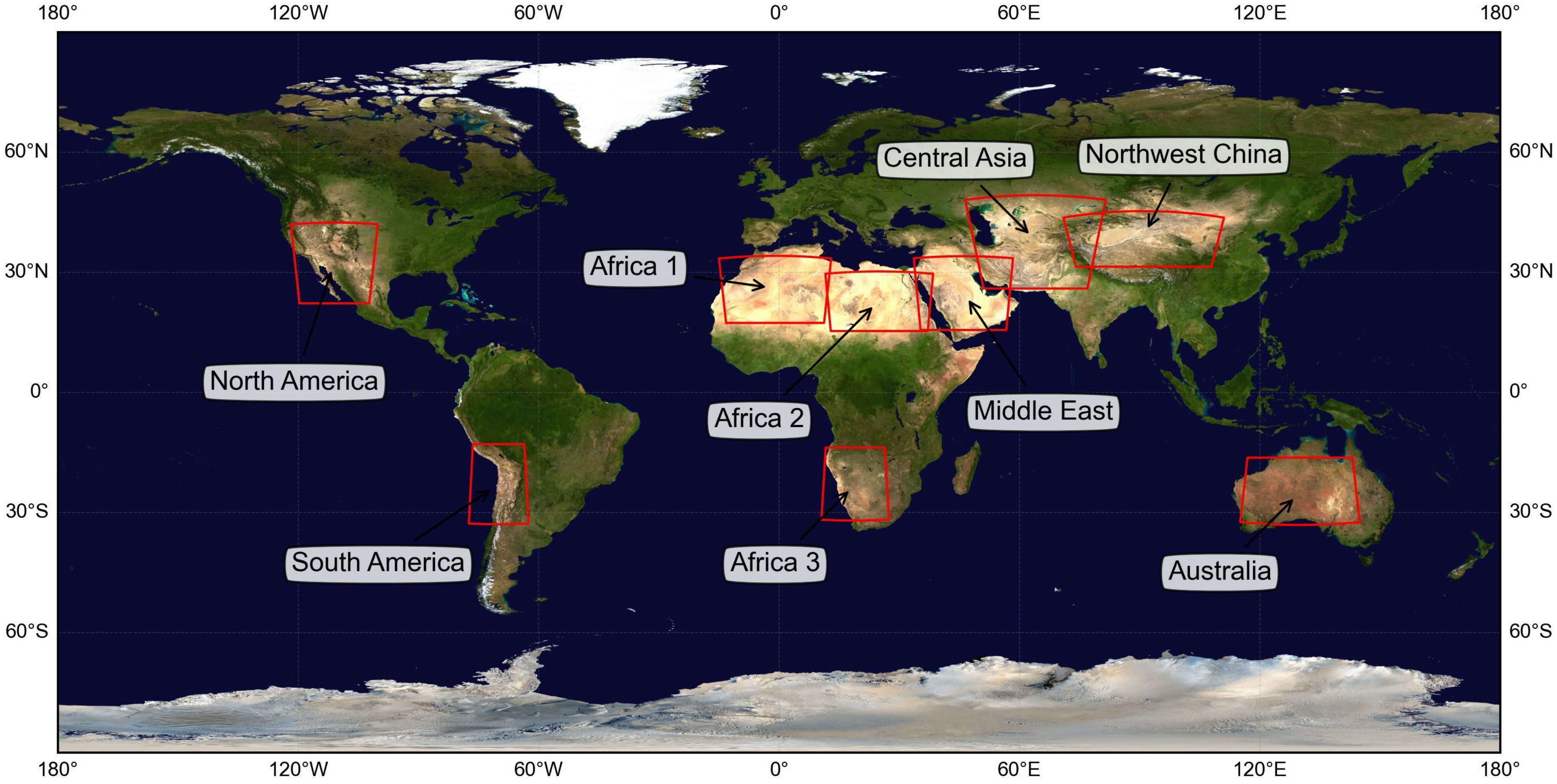

GPIPs distribution

The GPIPs align with traditional PICS, but additional hotspots areas were also identified, providing direction for subsequent selection of PICS.

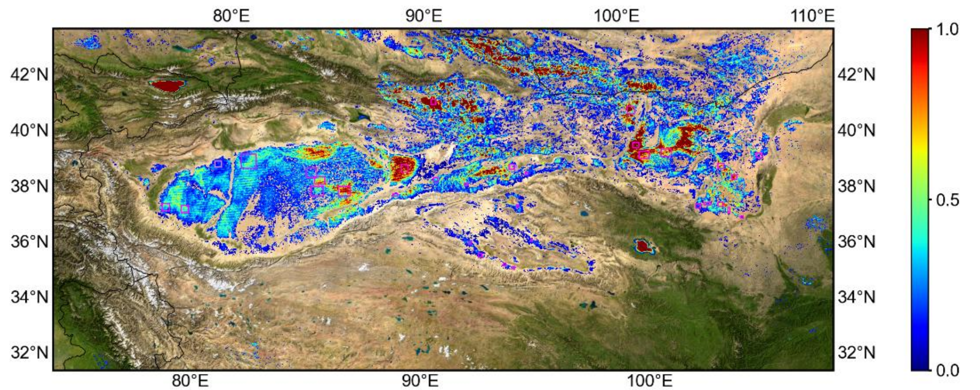

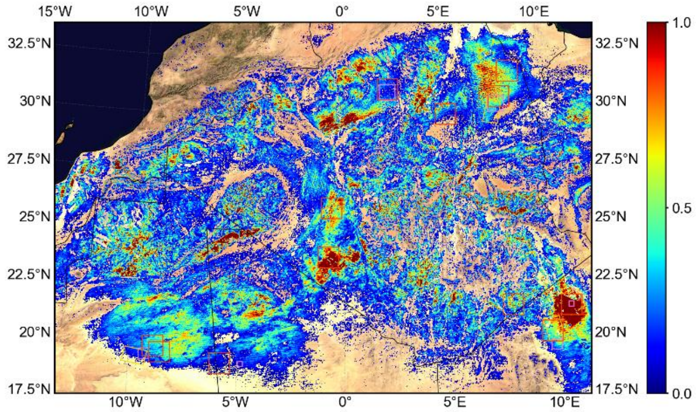

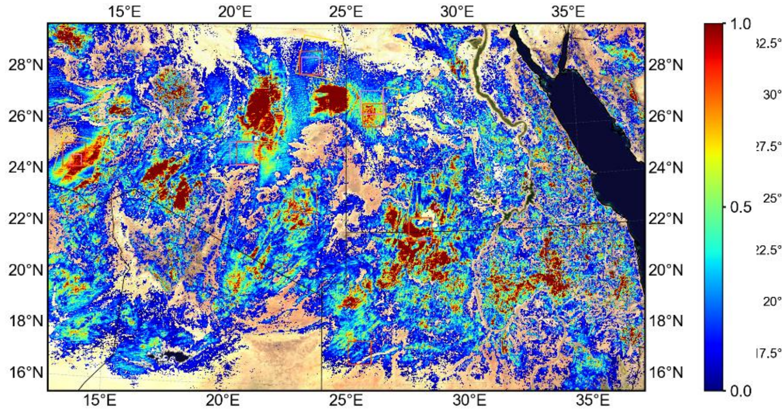

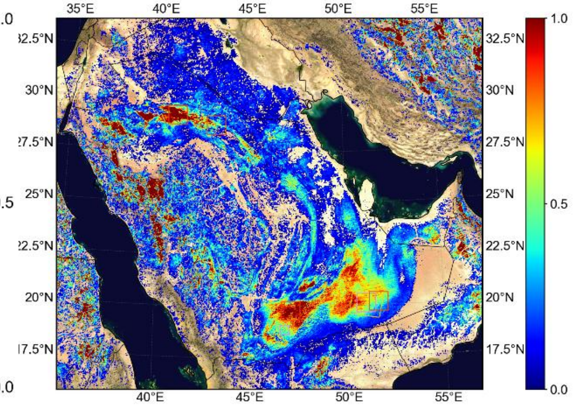

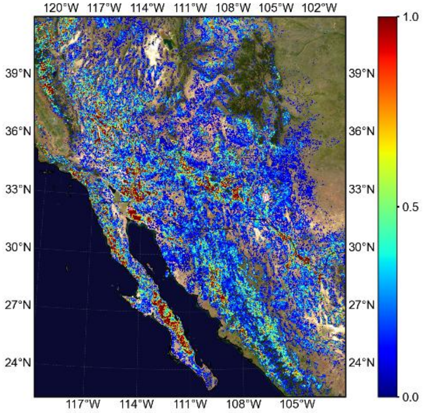

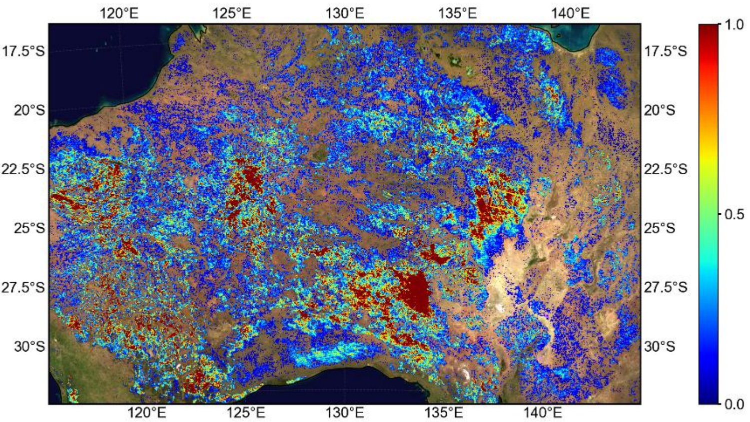

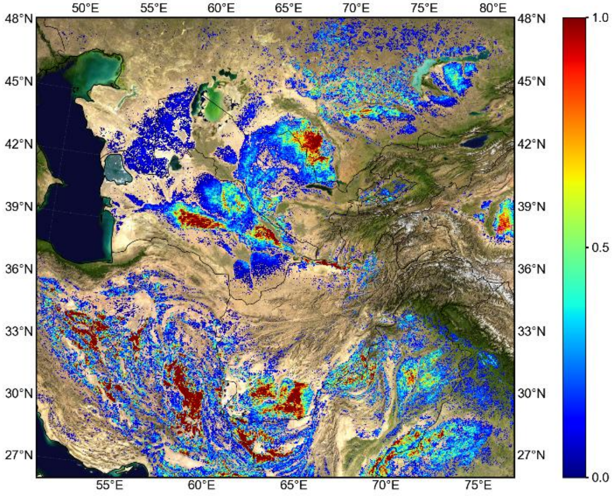

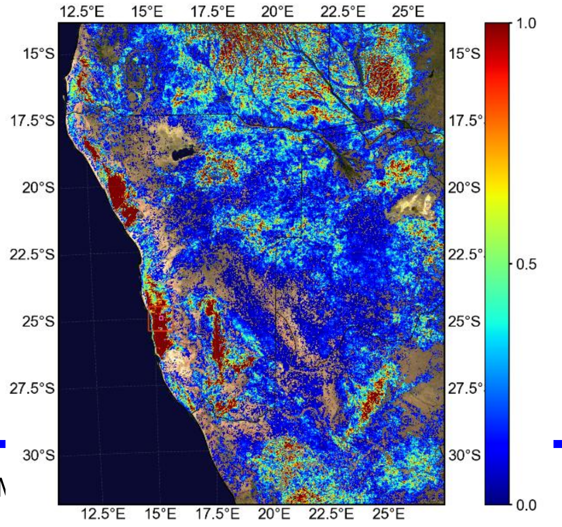

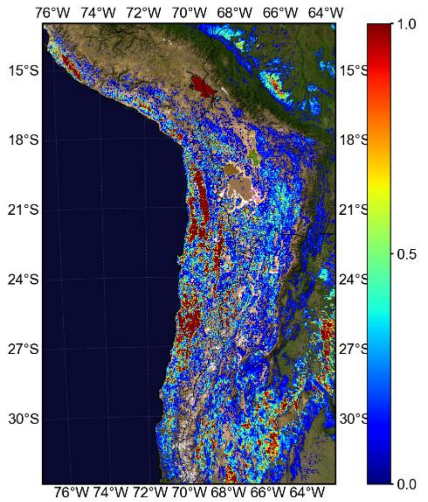

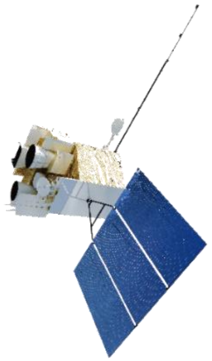

PART 02

Sensor inter-calibration based on PIPs

VIRR and MERSI-1 overview

Acronym	VIRR (FY-3)	MERSI-1
Full name	Visible and Infra-Red Radiometer	Medium Resolution Spectral Imager -1
Platform	FY-3A/3B/3C	FY-3A/3B/3C
Purpose	Multi-purpose imagery with emphasis on vegetation and ocean color	Ocean color, vegetation indexes and aerosol
Short description	10 VIS/NIR/SWIR/MWIR/TIR channels	20 channels, 19 narrow-bandwidth in VIR/NIR/SWIR and one broadband in the Thermal IR
Background	Similar to MVISR on FY 1C and 1D	New development
Scanning Technique	Cross-track: 2048 pixel of 800 m s.s.p., swath 2800 km - Along-track: six 1.1-km lines/s	Cross-track: 2048/8192 samples for channels at 1000/250m m resolution at nadir, swath 2900 km - Along-track: ten 1-km lines every 1.5 s.
Resolution	1.1 km at s.s.p.	250 m or 1.0 km at s.s.p.
Utilization Period:	2008 to 2022	2008 to 2021

satellite	VIRR		MERSI	
	band	CW	band	CW
FY3A	1	0.630	3	0.650
	2	0.865	4	0.865
	7	0.455	1	0.470
	8	0.505	10	0.490
			11	0.520
	9	0.555	2	0.550
FY3B	1	0.630	3	0.650
	2	0.865	4	0.865
	7	0.455	1	0.470
	8	0.505	10	0.490
			11	0.520
	9	0.555	2	0.550

IR-MAD technique for inter-calibration

Interest Region:

- mainly composed of desert, no vegetation, high reflectance thus high signal-to-noise ratio, and minimal atmospheric path effects;
- relatively arid with minimal atmospheric water vapor influence, and low occurrence of clouds and rainfall.
- spatially homogeneous, reducing spatial registration errors.
- relative smooth spectral profile (minimal impact when SRF varies greatly).
- two CEOS-endorsed PICS for validation.

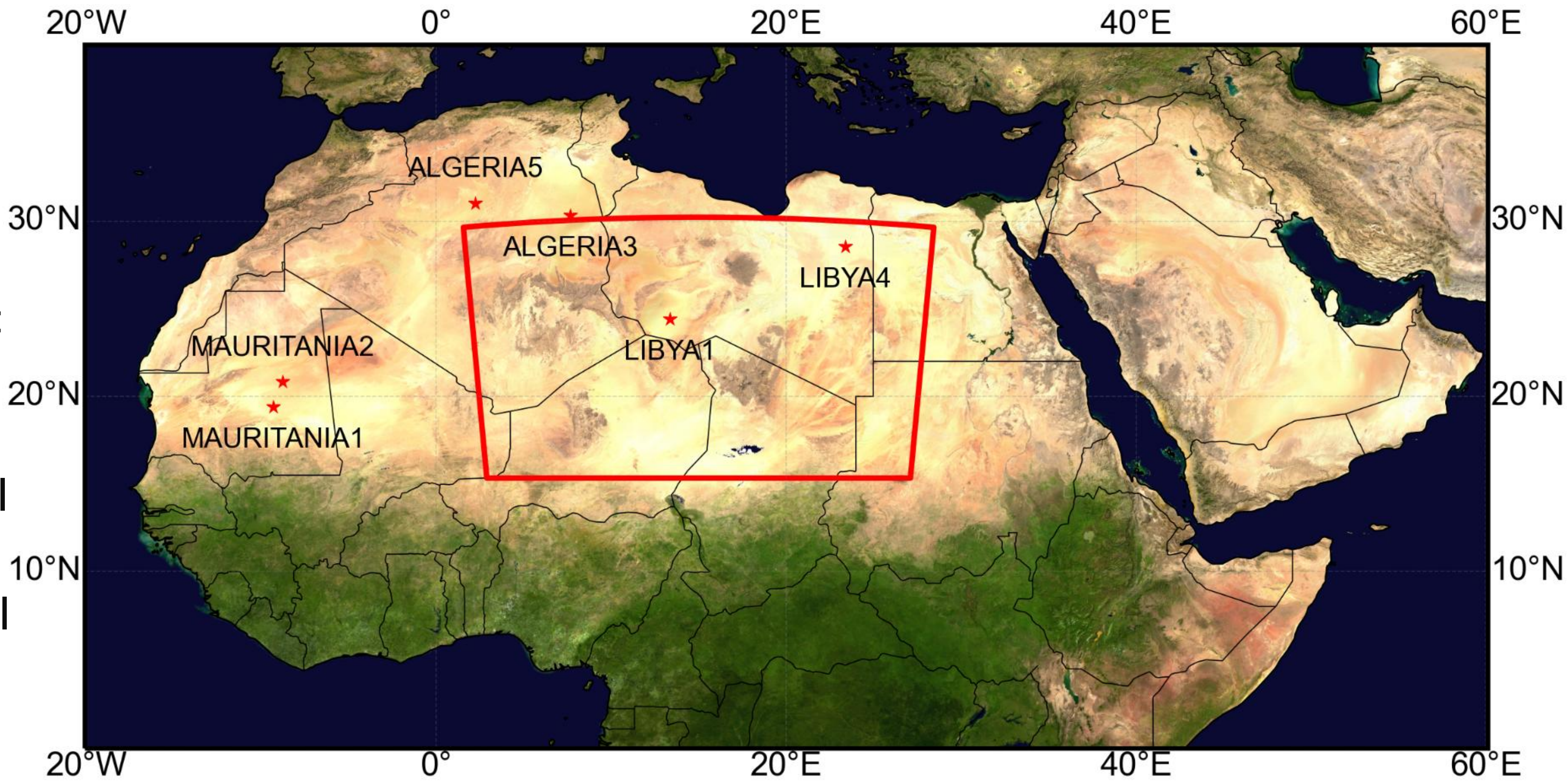

Data:

- FY3A-MERSI/VIRR L1B（20081112-20141231）
- FY3B-MERSI/VIRR L1B （20110121-20181114）

IR-MAD tech. for inter-calibration

Processing Flowchart:

1. Reproject the near-simultaneous overpass at the ROI from the two sensors onto a common geographic grid to get the image pair.
2. Mask out cloudy pixels (not strict) and pixels with sensor zenith angles greater than 30°.
3. Select pseudo-invariant pixels (PIPs) by the IR-MAD technique
4. Aggregate five consecutive days PIPs for regression
5. Perform an orthogonal regression on PIPs to get regression slope, which is a measurement of the intercalibration result.
6. Apply the above process to long-term data series, resulting in a long-term intercalibration result

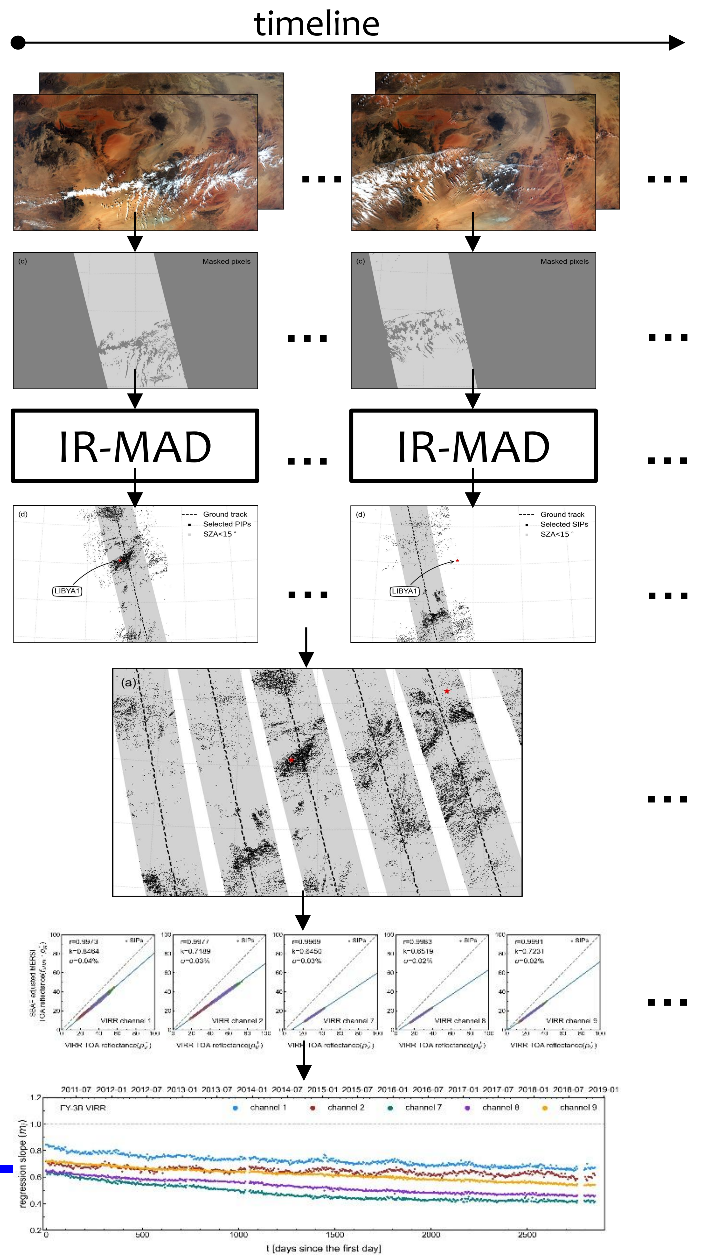

Spectral Band Matching SBAF

FY-3A/B band matching:

- VIRR：1、2、7、8、9
- MERSI：3、4、6、1、(10\11)、2

$$\overline{\rho}_{\lambda} = \frac{\int \rho_{\lambda} \mathrm{RSR}_{\lambda} d\lambda}{\int \mathrm{RSR}_{\lambda} d\lambda}$$

$$SBAF = \frac{\overline{\rho}_{\lambda}(VIRR)}{\overline{\rho}_{\lambda}(MERSI)}$$

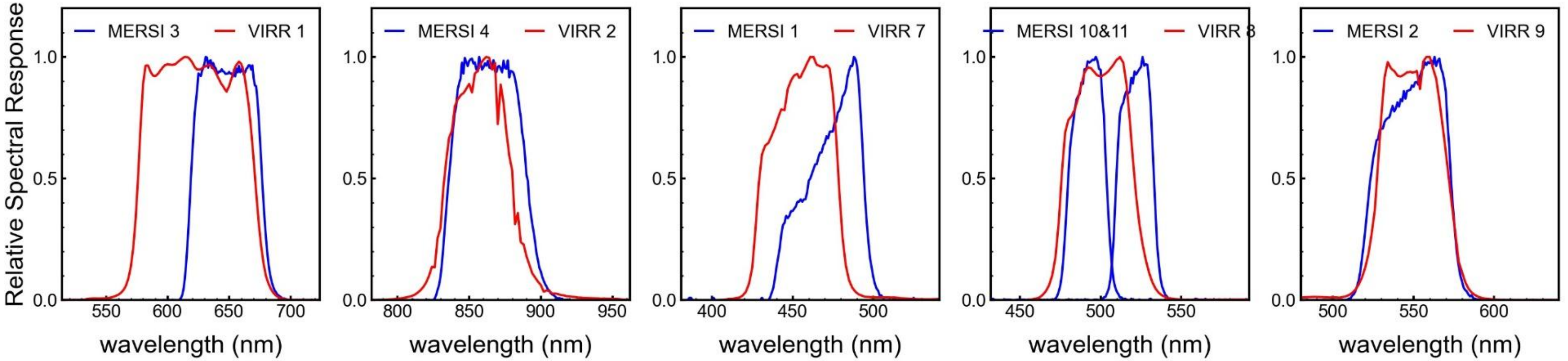

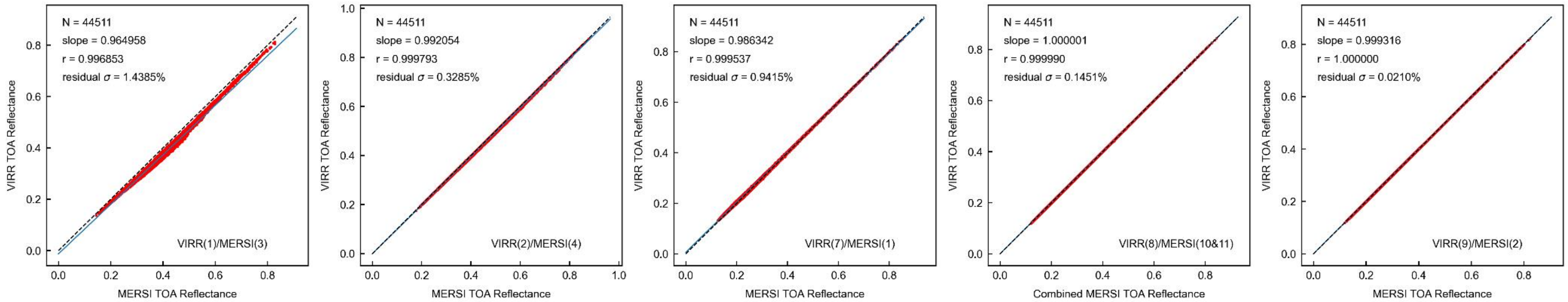

44,511 SCIAMACHY spectral samples were used for SBAF calculation, representing one full year of SCIAMACHY data within the ROI and encompassing the spectra of all surface types within the ROI (may also include cloud data).

Examples Applied on FY-3B

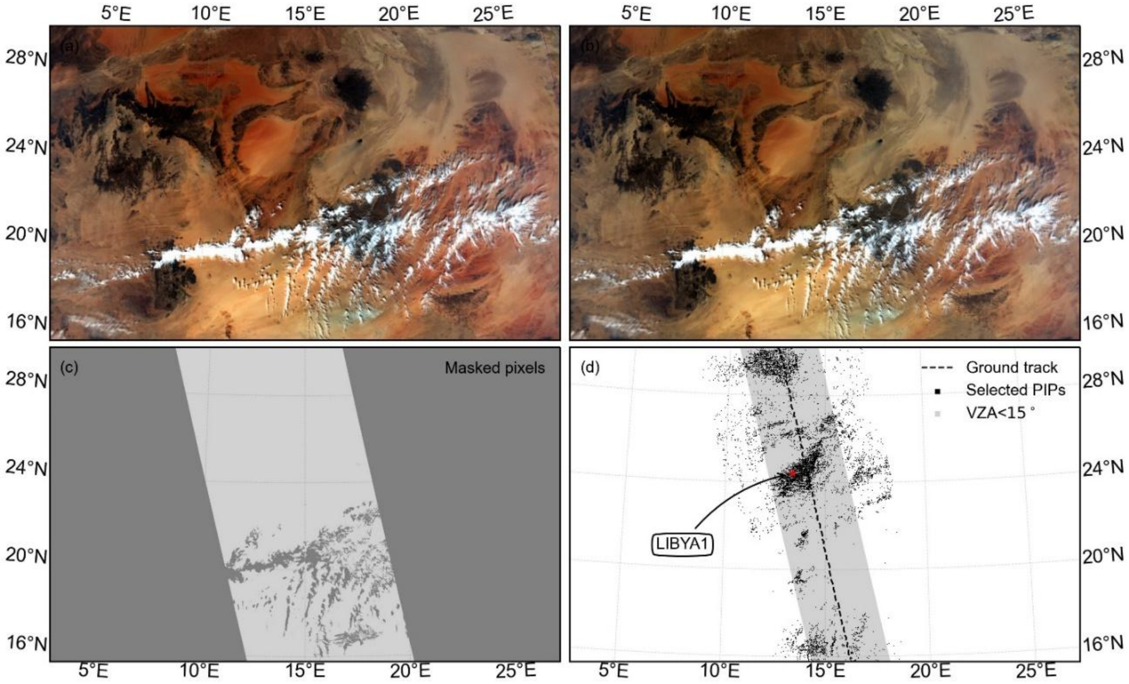

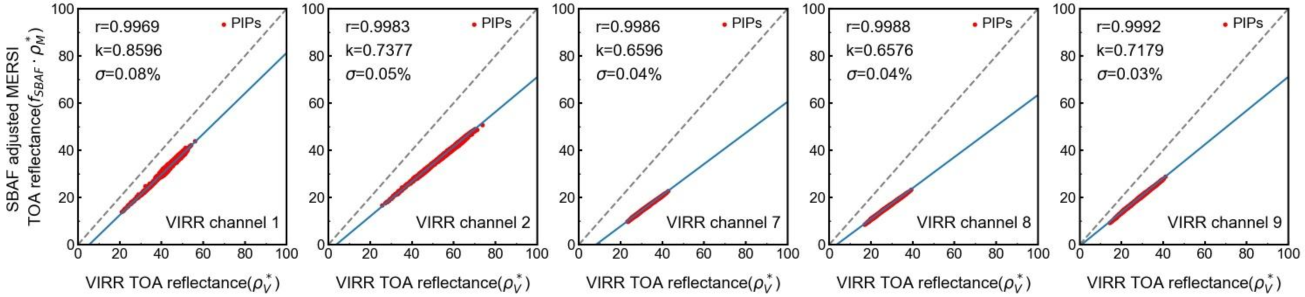

Regression results of PIPs from single-day comparison

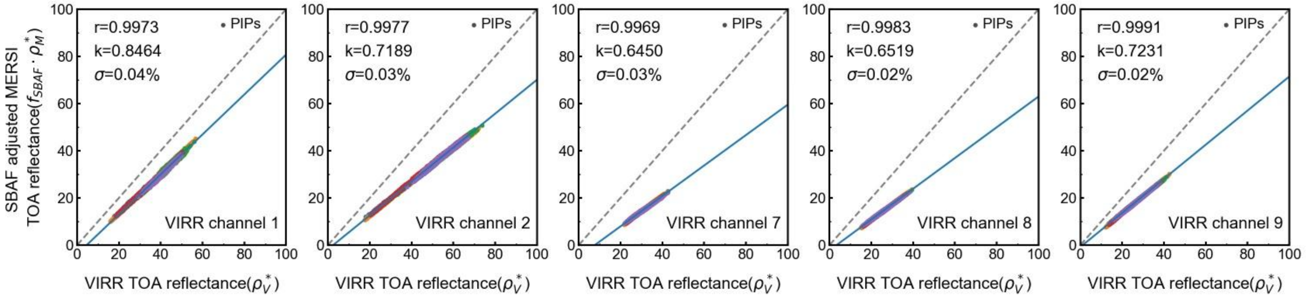

Regression results of aggregated PIPs from 5 consecutive days

Aggregate the PIPs from five consecutive days and perform linear regression.

1. Got a more stable regression
2. Richer samples, offering a higher dynamic range.

Examples Applied on FY-3B

Example of selected PIPs at early and later stage of FY-3B’s lifecycle:

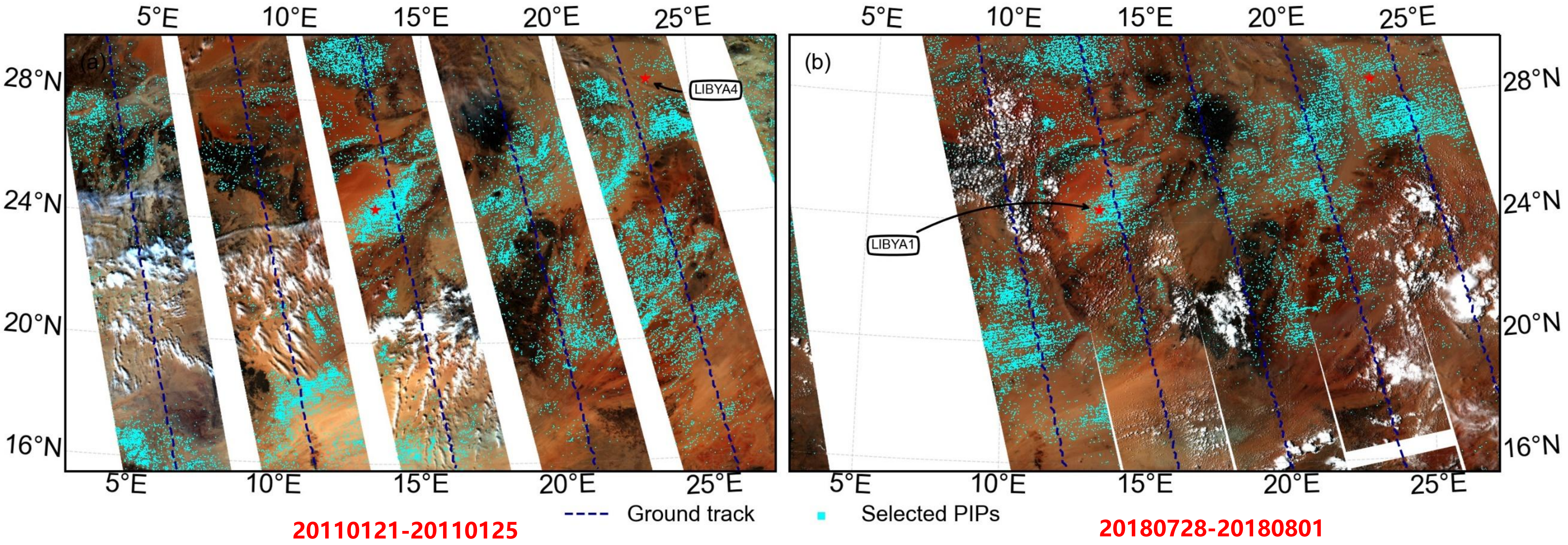

Although the orbit of the satellite has drifted during this period and the sensor has also experienced relatively large degradation, the spatial distribution of PIPs is consistent except in some cloud areas.

IR-MAD vs. SNO-x

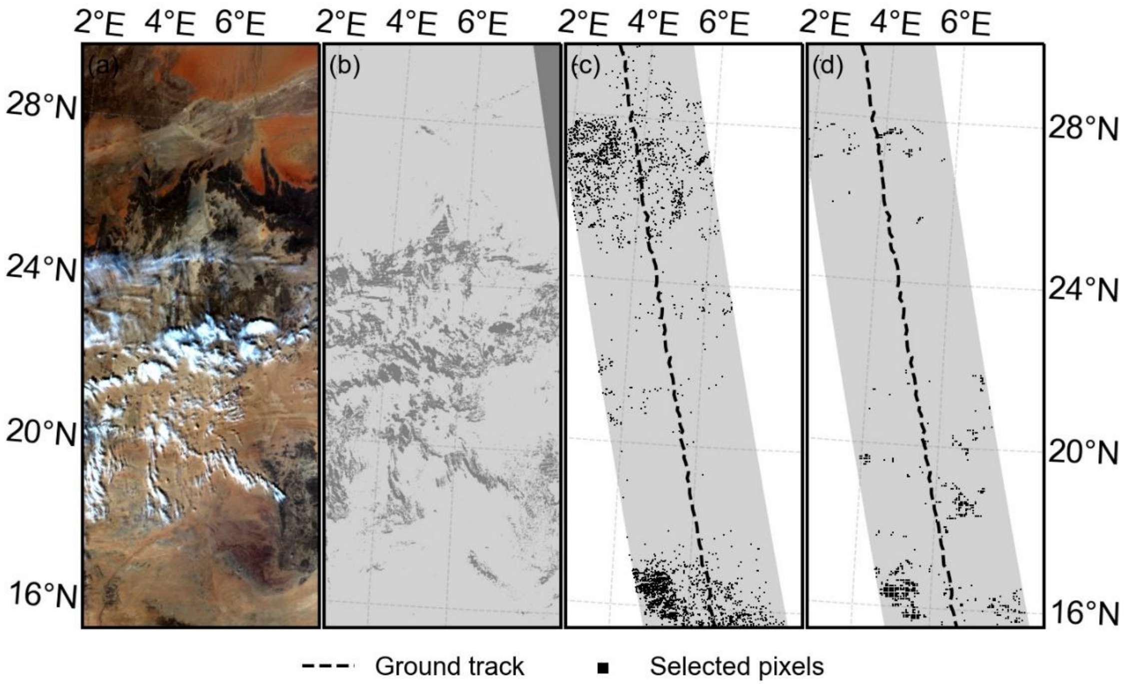

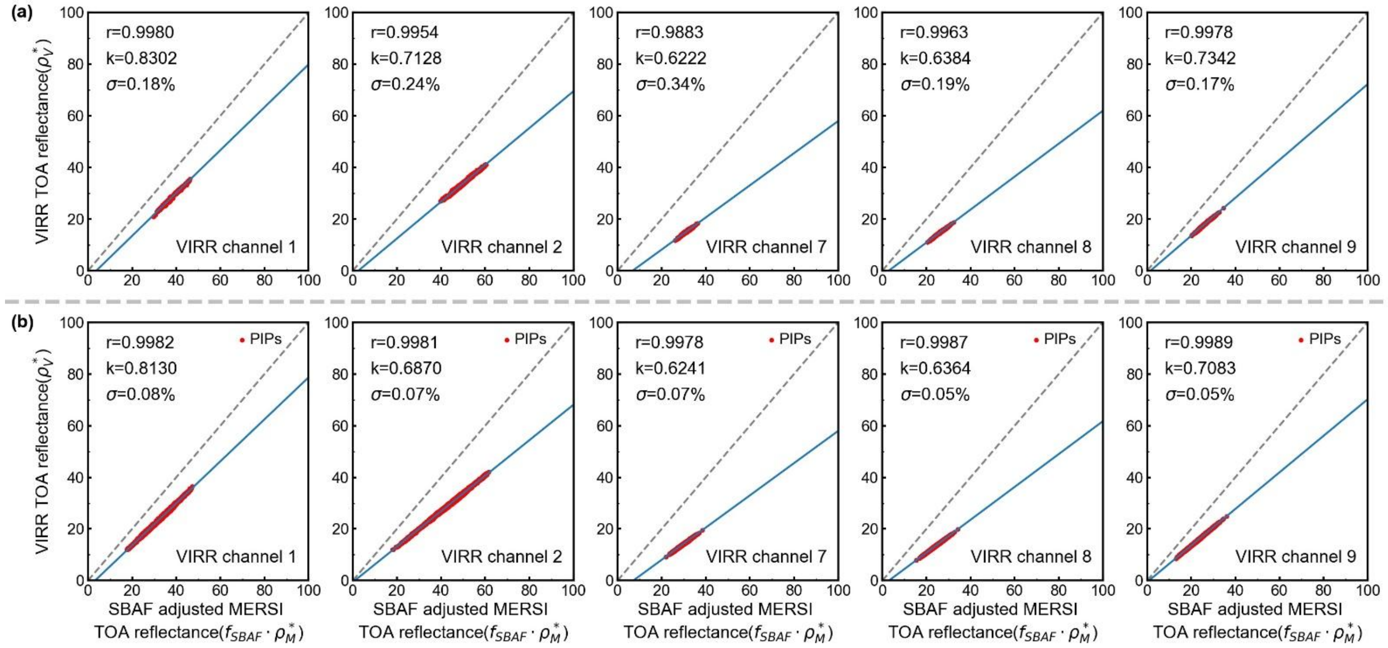

(c) IRMAD method. (d) SNO-x method. *(Uprety et.al, 2013)*

- IR-MAD selects samples requiring no prior knowledge of the surface
- **greater number of samples** compared with the SNO-x method
- offering **more diverse range of types** and a **wider dynamic range**.
- **SNO-x method sometimes fails**, particularly poor spatial uniformity, eg. northwest region of China.

Long-term Intercalibration Results

- The IR-MAD can provide a very stable long-term intercalibration results for both FY-3A and FY-3B
- One Inter-cal result per 5 days.
- Got the VIRR calibration trend if the Reference sensor MERSI is stable.

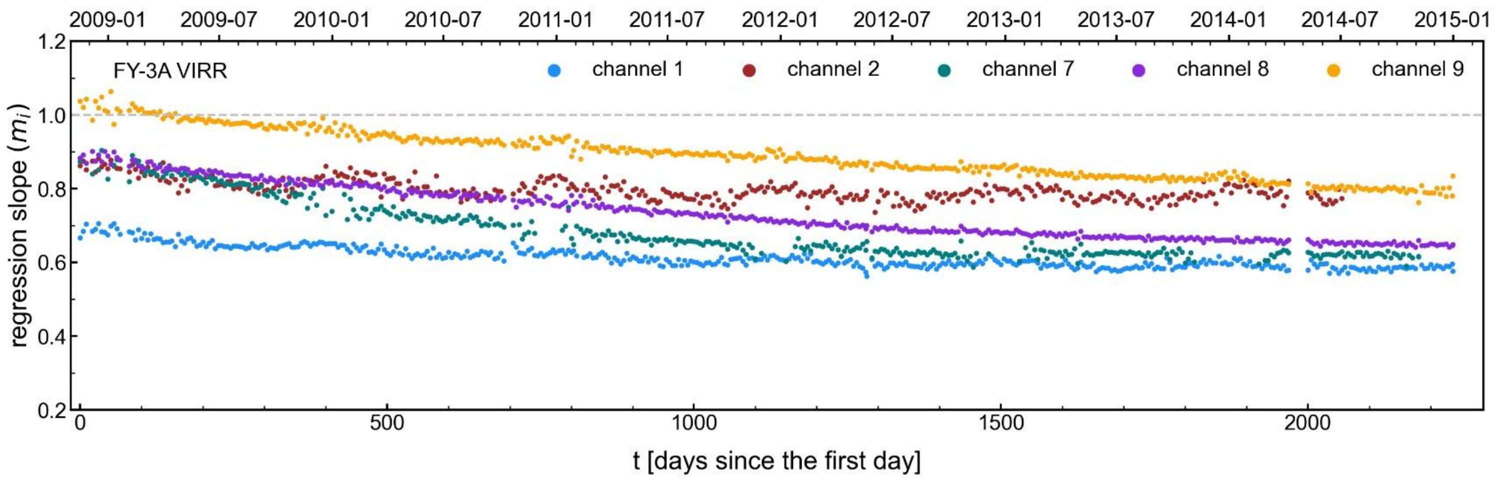

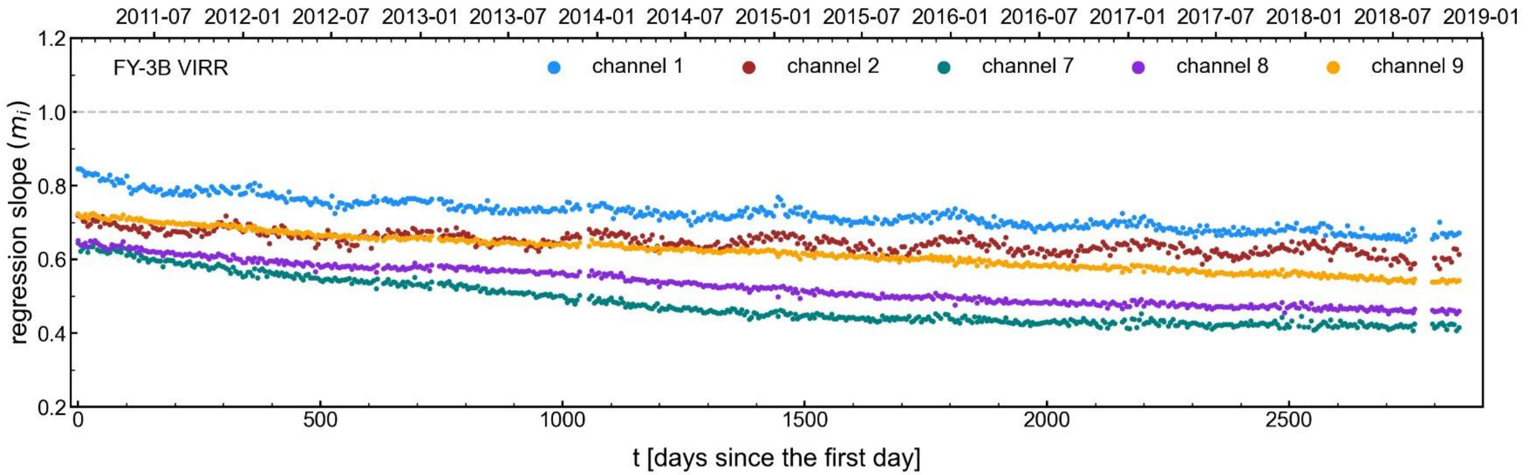

Long-term Trend Compared with other Methods

The obtained VIRR degradation results can be compared with those from other independent methods which show high consistency.

Solid line is inter-cal using PIPs, Dash Line from VIRR itself temporal Image pairs

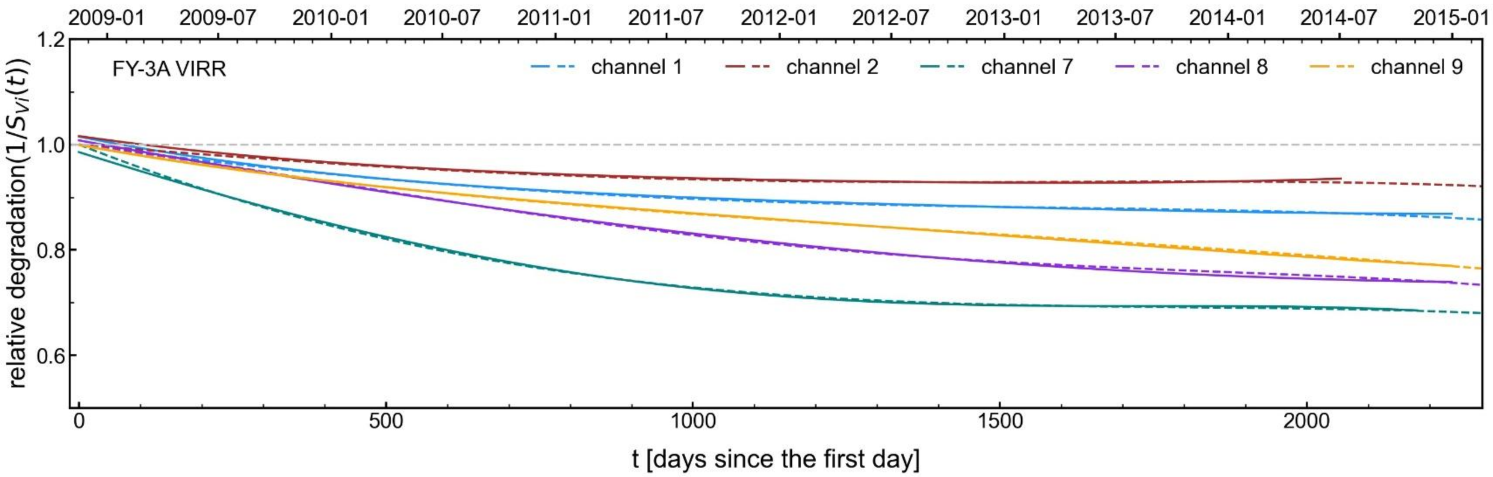

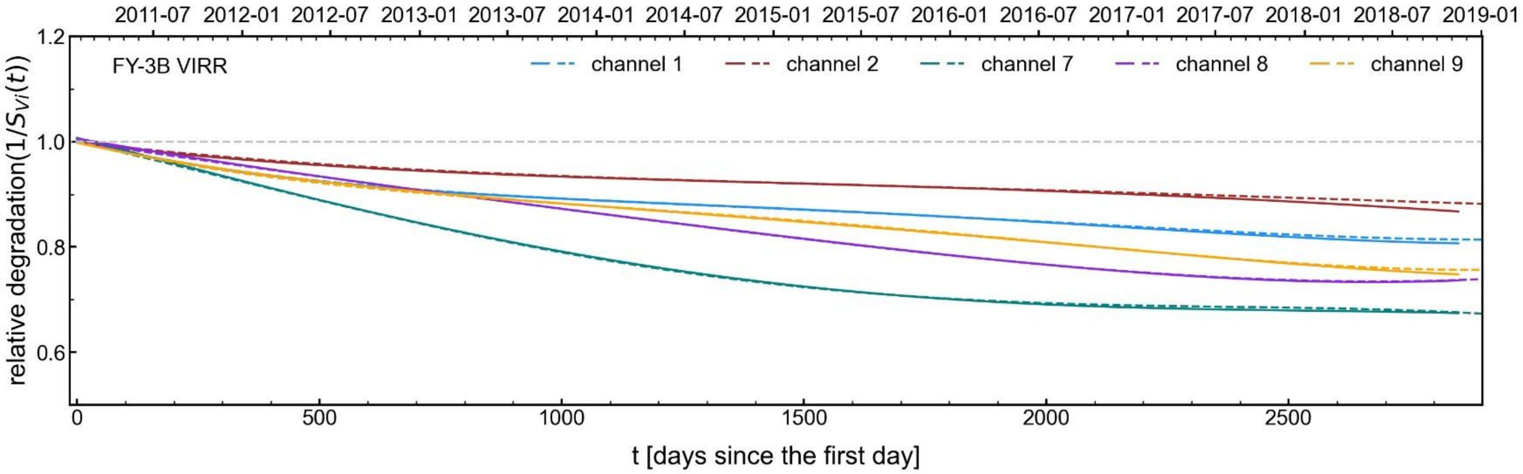

(*Wang et.al, 2019 in Chinese)*

Use LIBYA4 trend validation before/after interCal

FY-3A

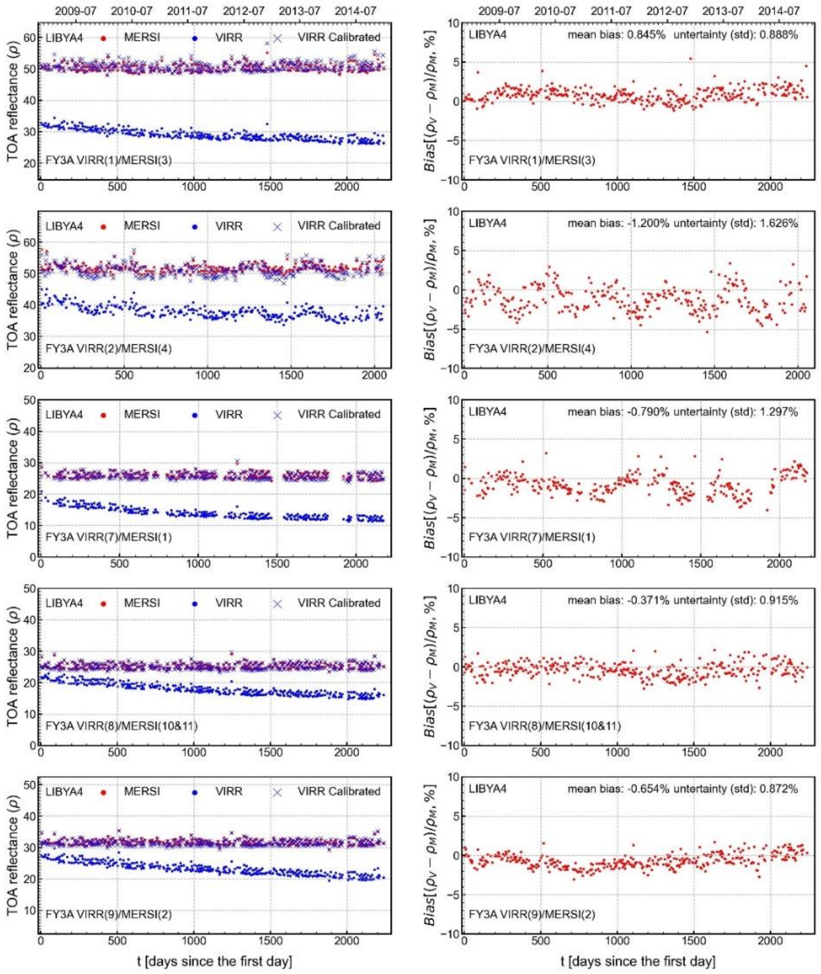

FY-3B

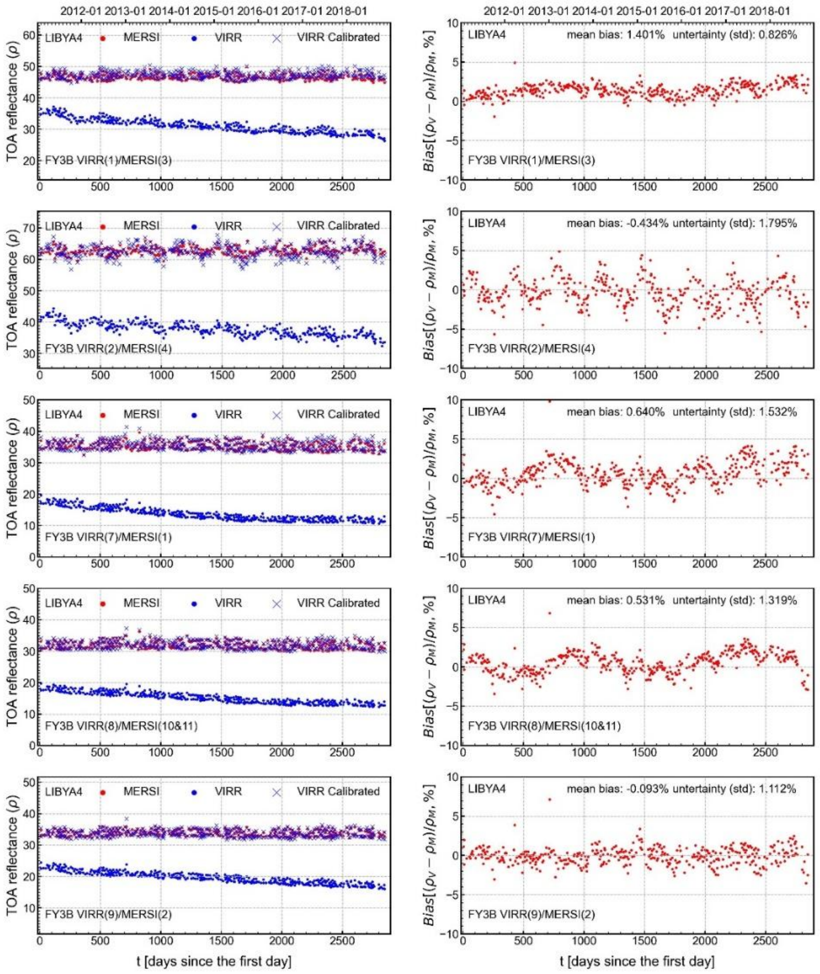

After inter-calibration, the trend of VIRR has been eliminated and it has a consistent radiometric response with MERSI, the bias mean <1.5%, std <2%.

Uncertainty Analysis

The uncertainty are analyzed from all the comparisons during the study period

	source	FY3A VIRR					FY3B VIRR				
		ch1	ch2	ch7	ch8	ch9	ch1	ch2	ch7	ch8	ch9
Uncertainty for image pair	misregistration atmospheric conditions BRDF effect spectral band differences	1.46%	1.30%	0.69%	0.68%	0.65%	1.50%	1.23%	0.85%	0.78%	0.89%
Uncertainty for long-term cross-calibration	polynomial fitting	1.64%	2.32%	1.83%	0.81%	1.05%	1.59%	2.31%	1.57%	1.28%	0.75%
	total error (root sum of squares)	2.20%	**2.67%**	1.96%	1.06%	1.24%	2.19%	**2.62%**	1.78%	1.50%	1.17%

- The IR-MAD can implicitly reduce uncertainty because it selects PIPs based on the potential linear relationship between the two images.
- The single SBAF obtained from all spectral samples in the ROI is the primary sources of uncertainty.
- When applied to sensors on different platforms, differences in overpass time and BRDF effects will introduce additional uncertainties, this can be reduced by more comparisons in more ROIs since the *mean effects tend to be zero.*

Spatial Distribution of PIPs using accumulated data

The density map of the spatial frequency distribution of PIPs for all image pairs of FY-3B

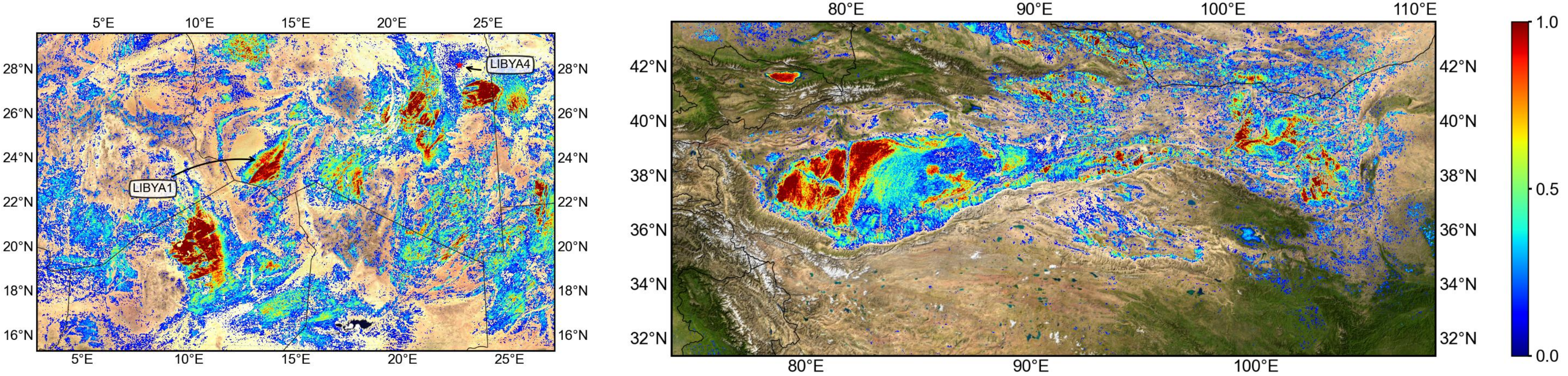

- We have conducted experiments on two regions, and obtained similar results
- in addition to recognized PICS such as LIBYA1 and LIBYA4 being found within the distribution area of PIPs, there are several extensive PIPs hotspot regions. These areas hold the potential to serve as valuable calibration sites for future research.

Applied on Sensors on Different Platforms

FY3B-Aqua SNO-x						
YMD	HMS(FENGYUN-3B)	Lat,Lon(FENGYUN-3B)	HMS (AQUA)	Lat,Lon(AQUA)	Distance(km)	Time_Diff(sec)
20110124	12:00:58	0.04 24.57	11:58:56	0.01 24.17	44.54	-122
20110503	12:33:44	0.04 16.23	12:29:34	0.02 16.50	30.16	-250
20110511	11:41:57	0.00 29.18	11:40:04	0.05 28.86	35.73	-113
20110519	12:31:40	0.04 16.74	12:29:25	0.04 16.52	24.91	-135
20110810	11:23:18	0.04 33.80	11:20:58	0.06 33.51	31.75	-140
20110818	12:12:55	0.05 21.39	12:10:19	0.01 21.18	24.25	-156
20111101	11:55:21	0.00 25.83	11:52:05	0.05 25.69	16.25	-196
20111109	12:44:47	0.01 13.48	12:41:17	0.00 13.40	8.65	-210
20120107	12:27:47	0.02 17.83	12:22:54	0.05 18.04	23.1	-293
20120306	12:09:46	0.04 22.49	12:04:44	0.05 22.67	20.6	-302
20120314	12:58:52	0.04 10.24	12:54:01	0.00 10.38	16.18	-291
20120504	11:50:55	0.04 27.40	11:46:38	0.04 27.30	10.91	-257
20120512	12:39:53	0.00 15.20	12:36:00	0.01 14.96	26.85	-233
20120624	12:23:47	0.00 19.40	12:16:58	0.00 19.65	28.13	-409
20120702	13:12:40	-0.00 7.21	13:06:36	0.00 7.23	2.36	-364
20120710	12:22:28	0.02 19.79	12:17:12	0.01 19.57	24.83	-316
20120901	12:43:57	0.04 14.61	12:35:23	0.01 14.97	39.68	-514
20121016	12:11:53	0.00 22.83	12:04:28	0.03 22.67	17.47	-445
20121130	13:20:42	0.04 5.85	13:12:22	0.00 5.72	15.16	-500
20121208	12:31:57	0.00 18.08	12:23:08	0.03 18.03	7.42	-529
20130401	12:21:11	0.04 21.50	12:11:39	0.01 21.08	47.35	-572

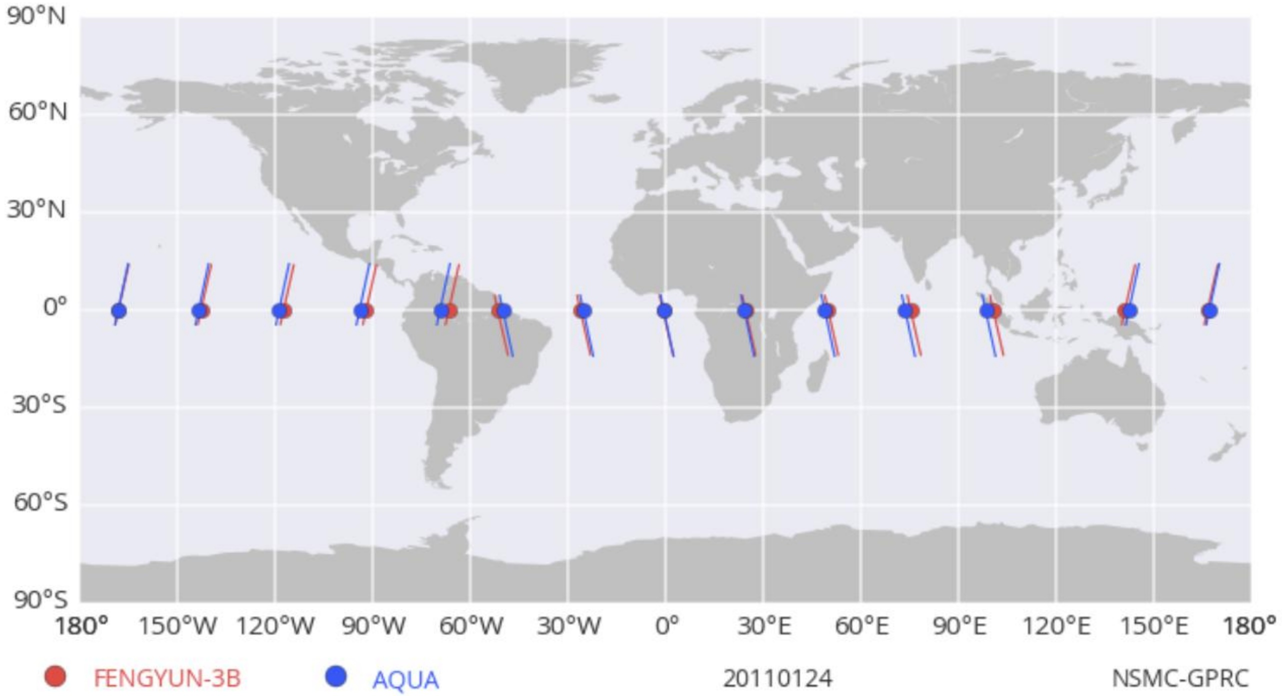

Matching bands

VIRR	1	2	7	9
MERSI	3	4	1	2
MODIS	1	2	3	4

Applied on Sensors on Different Platforms

intercalibrate FY-3B/MERSI Using Aqua/MODIS

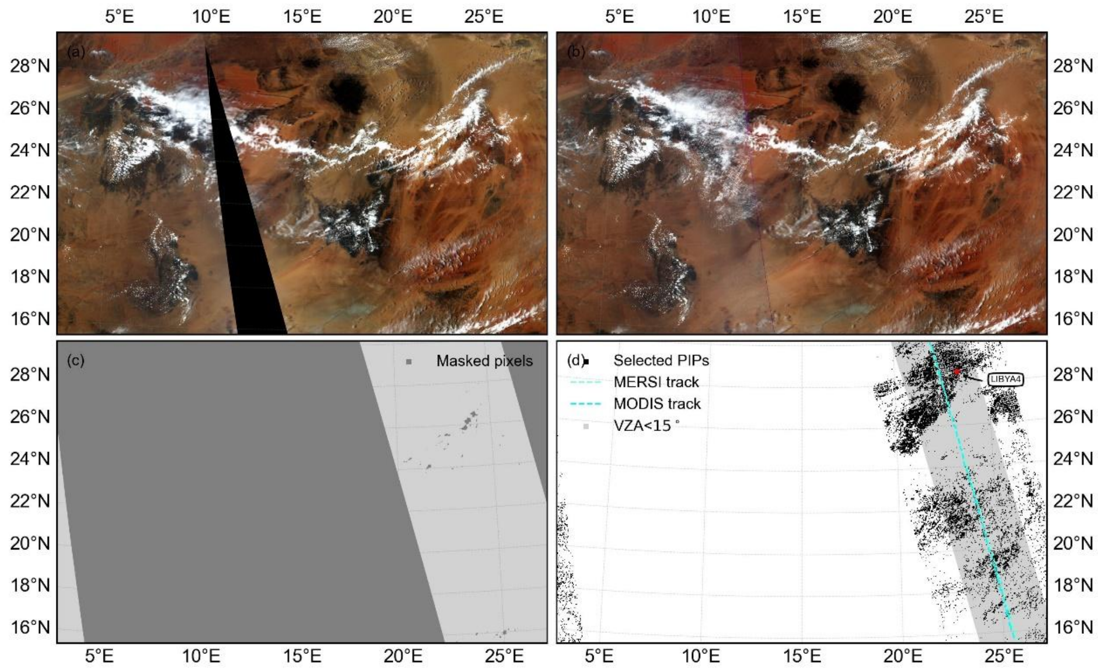

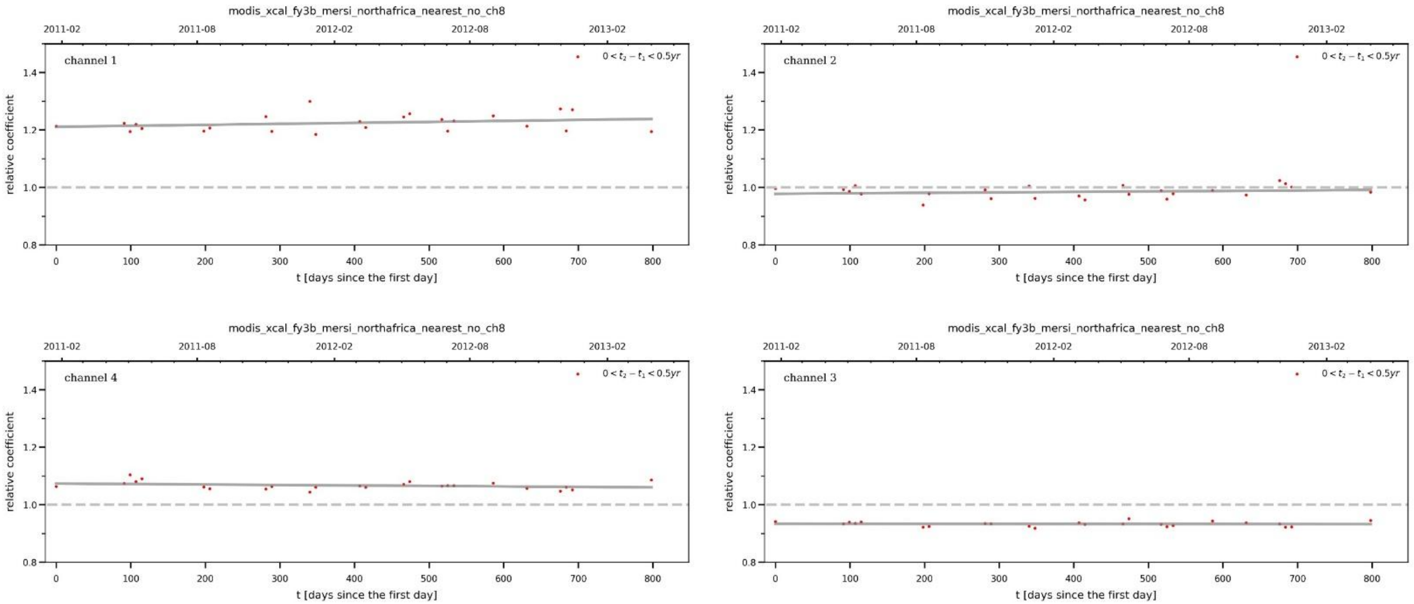

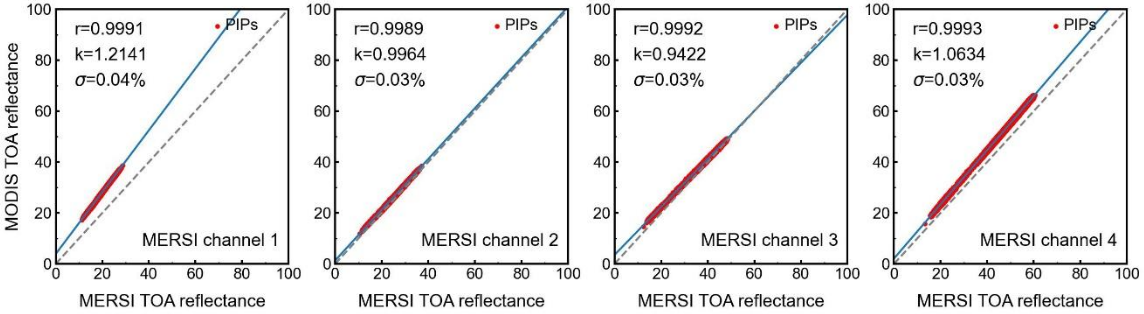

When applied to sensors on different platforms, differences in **overpass time and BRDF effects** will introduce additional uncertainties.

Inter-Calibration Transfer Chain

MODIS→MERSI→VIRR

Due to limitations of the on-orbit calibrator of MERSI, a calibration transfer chain can be established by inter-calibrating MERSI with MODIS, and then cross-calibrating VIRR with MERSI.

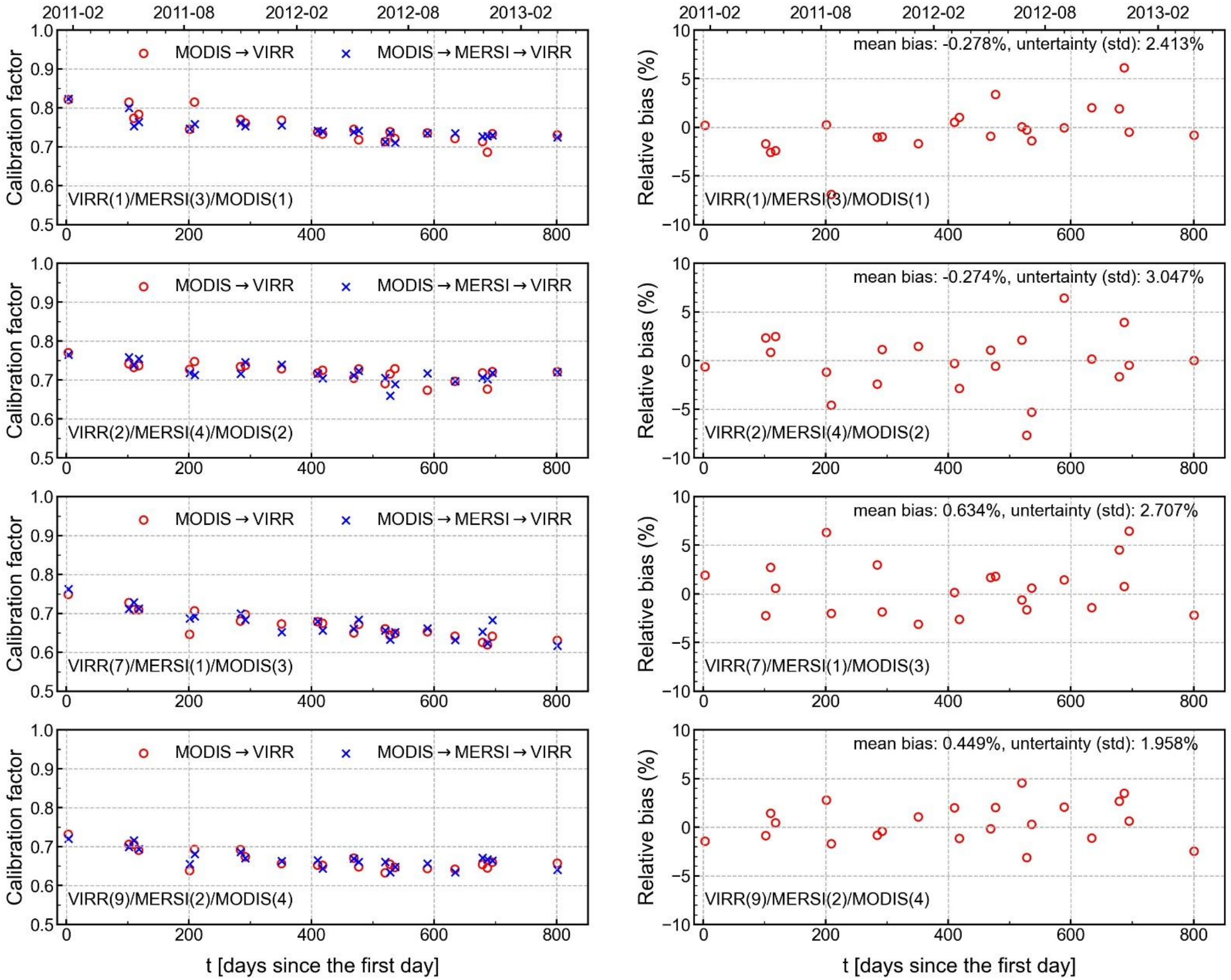

Inter-cal Testing between FY-3F/MERSI and Sentinel-3/OLCI

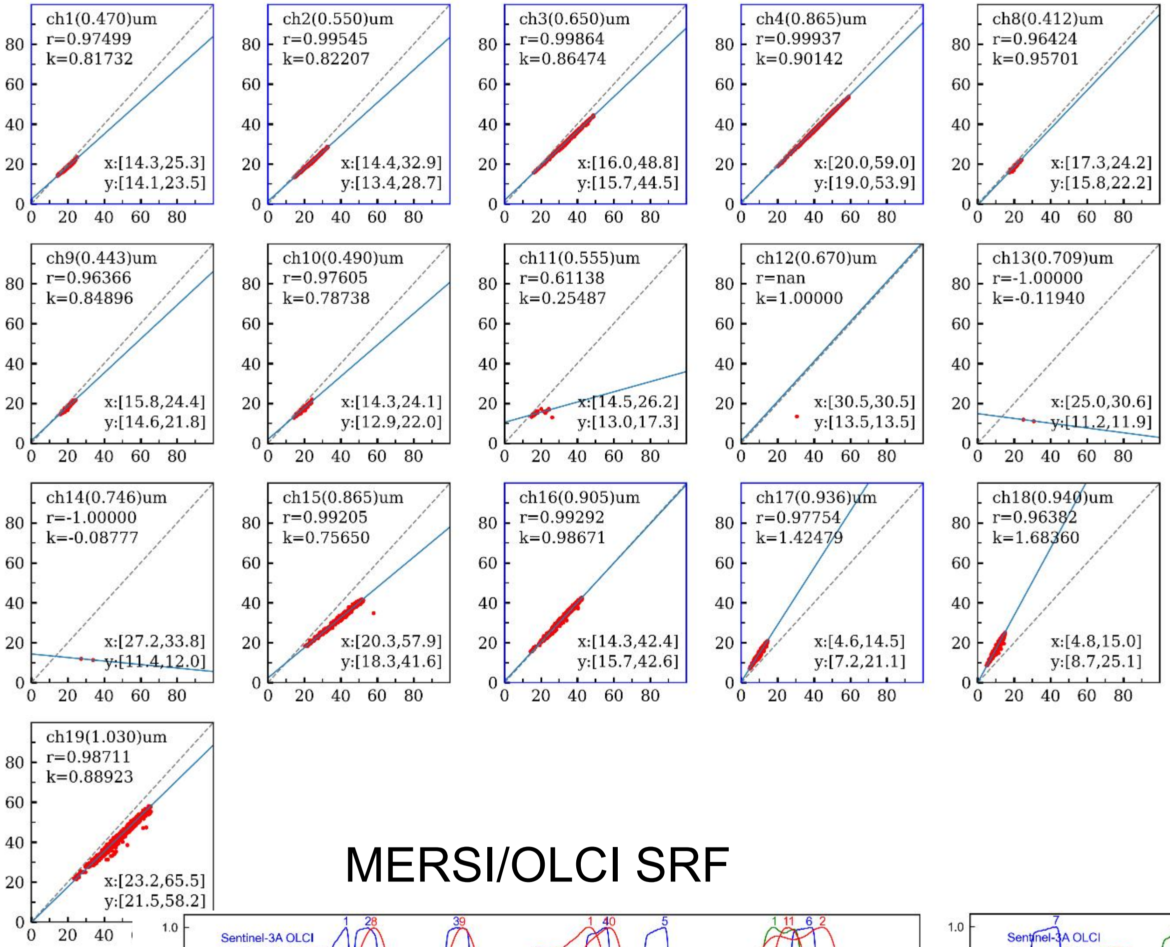

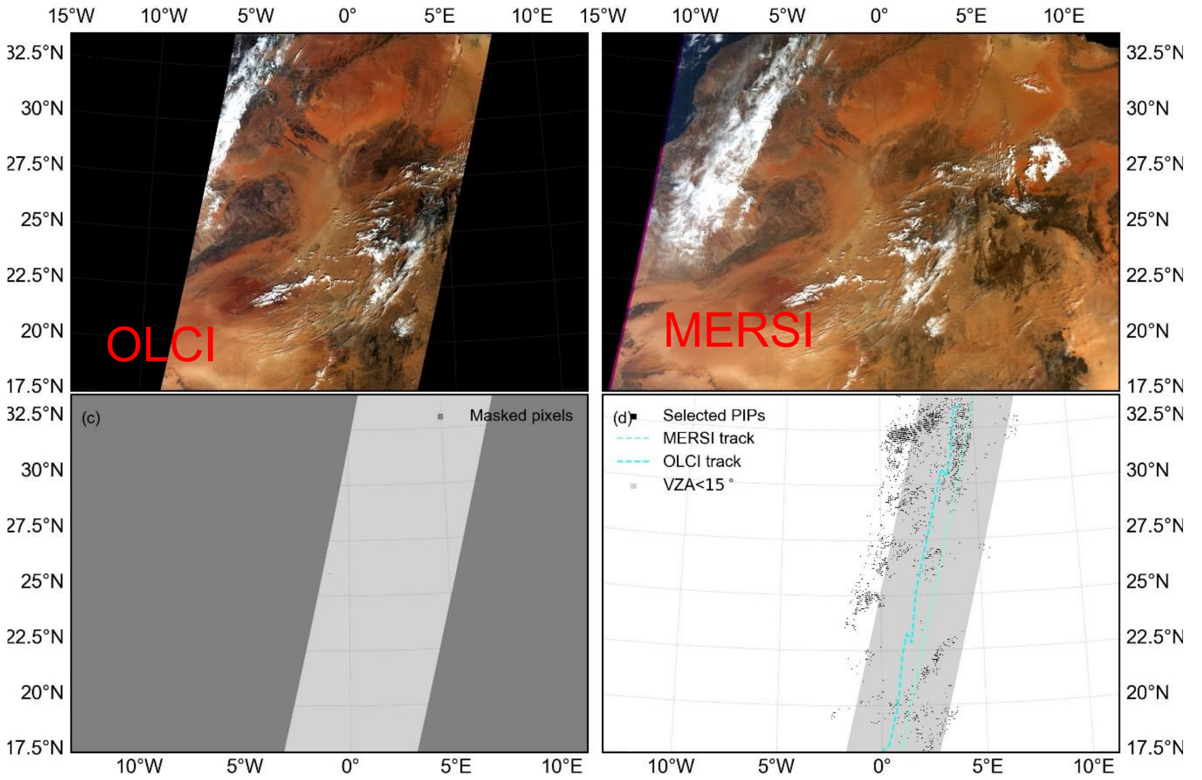

MERSI/OLCI SRF

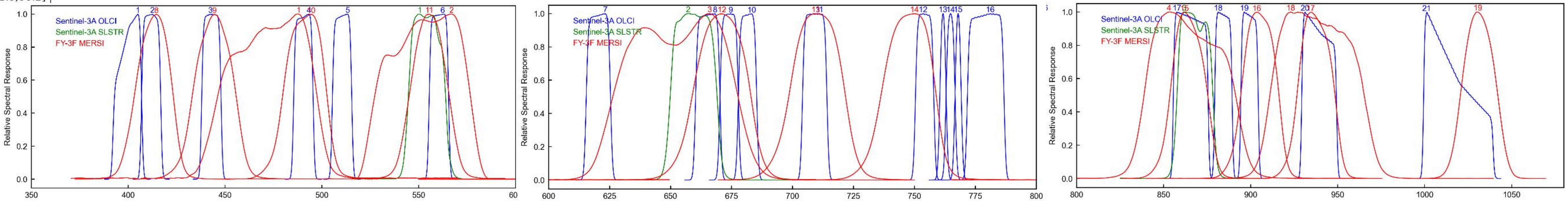

Inter-cal Testing between FY-3F/MERSI and Sentinel-3/OLCI

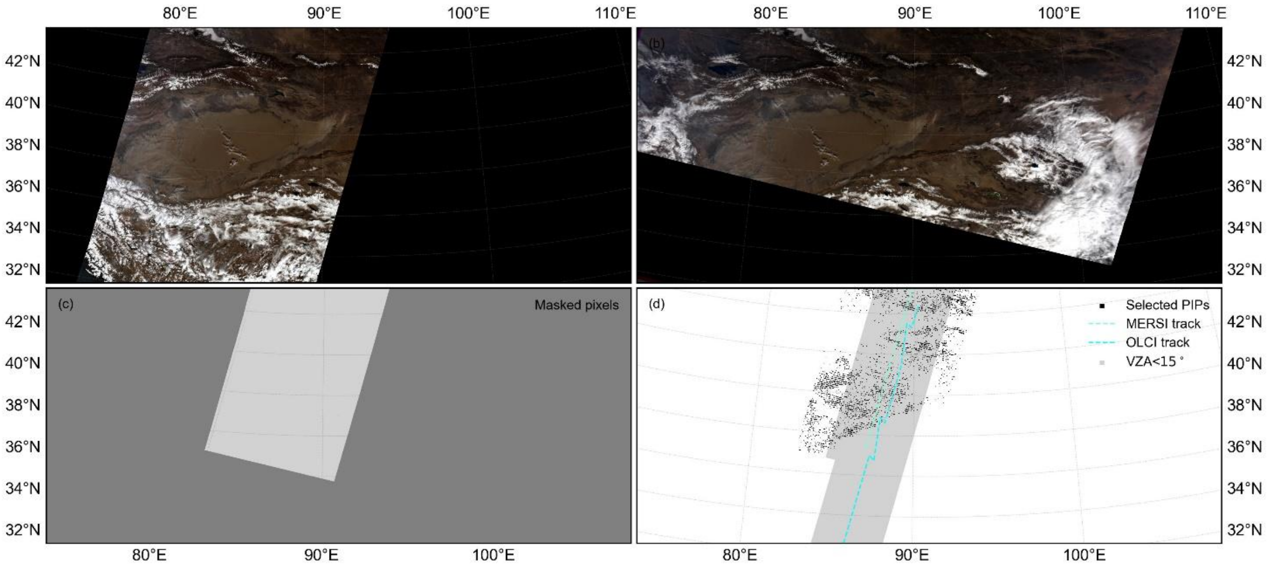

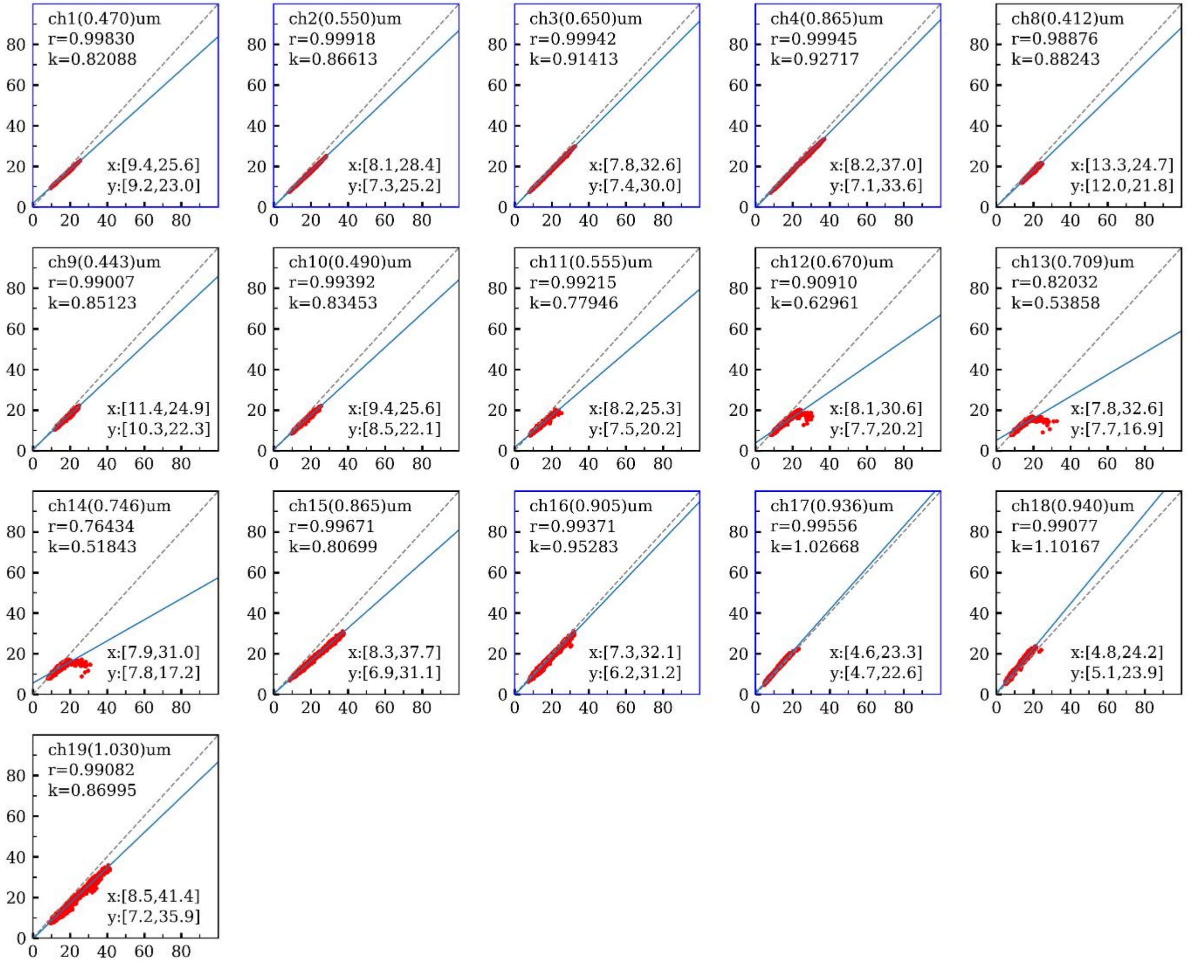

Conclusion and Way Forward

- The PIPs-based method is beneficial for the following purposes:
  - Intercalibration between sensor with similar bands
  - PIPs can be accumulated into PICS
  - Degradation trend monitoring
- PIPs extent traditional large-area spatially uniform PICS to the pixel level, allows for a more quantity of samples, richer surface types, and wider dynamic ranges.
- The large-scale distribution hotspots of PIPs indicate the direction for searching for other potential PICS.
- The identification of GPIPs requires no prior knowledge of surface properties, is not specific to a particular sensor, and is immune to the degradation of sensor itself.
- PIPs can reduce the uncertainty introduced by the atmosphere, geometry in the traditional calibration process, and can obtain more accurate and stable calibration results.
- Analyzing the Global PIPs (GPIPs), which will soon be featured in our upcoming work.
- CMA can share the experience and codes of this method and implement the practice in the next step within GSICS community

Thanks for your attention!